8-9-2006

Fabrication and Magnetic Property Investigation of Metallic Nanowire Arrays

Bo Ye
University of New Orleans

FABRICATION AND MAGNETIC PROPERTY INVESTIGATION OF METALLIC NANOWIRE ARRAYS

A Thesis

Submitted to the Graduate Faculty of the
University of New Orleans
in partial fulfillment of the
requirements for the degree of

Master of Science
in
The Department of Chemistry

by

Bo Ye

B.S. Zhejiang Normal University, China, 2000

August 2006

ACKNOWLEDGMENTS

First I would like to express my sincere appreciation to my research advisor, Professor John B. Wiley, for his invaluable guidance and support throughout my graduate studies. Without his encouragement, this work would have never been done. Thank you very much, Professor Wiley.

I would also like to thank Professor Leonard Spinu for his generous help in characterizing magnetic properties and analyzing magnetism spectra during my all research work.

I would like to thank Professor Jiye Fang for his help on my graduate research and his constructive suggestions in revising my dissertation.

I sincerely thank Professor Guijun Wang and Professor Mark L. Trudell for their help, direction and invaluable encouragement during my graduate studies.

I would also like to thank Professor Weilie Zhou for his help in scanning electron microscopy characterization.

I would thank Dr. Dorin Cimpoesu in Prof. Spinu's group for his generous help in magnetic property measurements.

I would also like to thank everyone in Dr. Wiley's group for their help, advices and friendship in the past two and half years.

Table of Contents

Abstract

Single Metallic Nanowire Arrays (Ni, Au and Cu *etc*) and superlattice nanowire arrays (Ni/Au, Ni/Cu) were synthesized through template-directed electrochemical deposition method. The dual-bath technique was employed in fabrication of superlattice nanowire arrays. Anodized alumina membrane (AAM) and Ion Track-etched Polycarbonate Membrane was used as the fabrication templates. The specific electrode making technique and electrochemical deposition procedures were described in detail. Scanning electron microscope (SEM) performed all sample characterization. Vibrating sample magnetometer (VSM) and ferromagnetic resonance (FMR) were utilized to investigate the magnetic properties of single Ni nanowire arrays of different lengths and Ni/Cu superlattice nanowire arrays. The VSM data exhibited that the magnetic easy axis of samples is parallel to the nanowire axis direction and the nanowire arrays have obvious shape anisotropy. The FMR spectra indicated that the resonant field value is angular and aspect ratio dependence.

Chapter 1

Introduction

1.1 Significance of Synthesis of Metallic Nanowires and Magnetic Property Study

Nanoscience and nanotechnology is one of the main directions of advances in science and technology in the 21st century, which comprises scientifical and technological developments on the nanometer scale, usually locate between 1 and 100 nanometer. When the new materials and devices are fabricated in this characteristic scale, lots of unique properties and performances could be achived in this atomic-scale architecture system. As we known, the technological revolution always built on the foundation of advanced materials and advanced manufacturing. Nanostructed materials as a category of advanced materials are the foundation of nanoscience and nanotechnology. Moreover, the nanostuctured materials is also needed in advanced device fabricaton and system self-assembly. Generally, the research in nanomaterials includes four main fields: 1) Structurally controlled nanomaterial fabrication; 2) Characterization of the nanomaterial structures and properties; 3) Device fabrication; 4) System Manufacturing. All in all, research in nanomaterials needs multidisciplinary efforts among physicists, chemists, material professionals and mechanic engineers etc.

In the past few years, much of the progress in synthesis, structure characterization and physical property investigation for nanomaterials with reduced dimensionality, such as two-dimensional quantum wells[3,4,9,10,11] or nanofilms[12,13,14], one-dimensional nanowires[15,16,17,18,19,22], nanotubes[1,20,25], or nanobelts[21,23,24] etc. and zero-dimensional quantum dots[5,6,7,8], has been achieved. The two most important examples are: 1) In 1991 Dr. lijima first fabricated one-dimentional carbon nanotubes[1]; 2) In 1985, Richard E.

Smalley from Rice University discovered the Fullerenes (C_{60})[2], which brought him the Nobel Prize in Chemistry 1996.

Based on the material properties and utilization, one-dimensional nanowire systems can be classified as semiconductor compound nanowires [26,27]; Silicon [28,29] and germanium [30] nanowires; Oxide [31], carbide [32,33] and nitride [34] nanowires; and metallic nanowires [15,16]. In this thesis, we will only concentrate on the metallic magnetic nanowires. In the past few years, metallic nanowires have aroused a remarkable interest due to their potential applications in giant magnetoresistance (GMR) effect based magnetic sensor [37,39,40], ferromagnetic nanowires based tunable microwave filters [35,36] and magnetic recording media [38,41] etc. It is not difficult to see that almost all above potential applications of metallic nanowires are based on their magnetic properties. Therefore, the investigation of the efficient large-scale synthesis methods of different metallic nanowires and their diverse magnetic properties are the key to approach their practical application in the near future.

1.2 Template-Directed Electrodeposition Approach

Much of the progress in the fabrication of nanowires has been achieved in the past few years. Lots of novel methods have been developed for synthesis different types of nanowires. The most commonly used nanowire preparation techniques include four aspects as listed below: 1) Vapor Phase Evaporation [43,44,45,46]; 2) Chemical Vapor Deposition, developed by Wagner and Ellis in 1964 for whisker growth [42]; 3) Laser Ablation [47,48,49]; 4) Electroless and Electrochemical Deposition [15,16,17]. For the synthesis of metallic nanowires, the electrochemical deposition technique has been approved a very

efficient way to produce high quality and large-scale nanowires. Therefore, this technique has been used widely recently. Initially, the electrochemical deposition technique was developed for decorative purpose in industry. Then, this technique was also found has many other engineering application in wear resistance and corrosion protection *etc*. Before this technique was utilized to make nanowires, it has been also widely used to make nanofilms and coatings on appropriate substrates [50,51,52]. In 1996, Martin became the first scientist to investigate the electrochemical deposition technique for metallic nanowire preparation in nanopore template of polycarbonate membranes [15]. Then Wang *et al* [16] and Peng *et al* [17] began to use this technique for synthesis of different metallic nanowires. For metallic nanowire growth using electrochemical deposition technique, we also have to apply with template-directed technique. If there has no template-directed technique to be applied, it could not be realized for nanowire preparation by just employing electrochemical deposition. Generally, the approach for making metallic nanowires based on template-directed electrochemical deposition technique includes three steps: 1) Formation of nanometer-sized channels in appropriate membranes; 2) Electrodeposition of metallic nanowires into the nanometer-sized channels using membrane as template; 3) Post-Treatment of the metallic nanowires.

1.2.1 Template-Directed Synthesis

Template-Directed synthesis is the most commonly used approach in our nanomaterial research. This technique is also called the bottom-up approach by comparison with top-down approaches, such as X-ray lithography and focused ion beam (FIB) [61]. However, both the lithography and FIB techniques are comparatively cumbersome and expensive

for large-scale fabrication. Therefore, researchers are of great interests in the template-directed synthesis currently. Template-directed nanomaterial fabrication method also has some other advantages: 1) This technique becomes a “bridge” linking microscopic world (nanowires, nanotubes and nanorods etc nanometer-sized structures) to the current macroscopic world (different types of membrane templates and electrochemical deposition); 2) Good reproducibility; 3) Shape of nanometer-sized structures are pre-designed; 4) The fine microscopic tips (such as atomic force microscopy (AFM) and scanning tunneling microscopy (STM)) are not a must any more in the manipulation of the nanomaterial building blocks.

1.2.1.1 Templates

Anodized alumina membrane (AAM)[53] and ion track-etched polymer membrane [54] are the most commonly used as fabrication templates. Both of these two types of membranes are commercially available. The main provider of these two types of membranes is the Whatman Company. Initially, these two types of membranes were developed for lab filtration applications because they occupy relatively precise pore structure and narrow pore size distribution, which is suitable for filtrate certain sized material and biological particles. The first person utilized these types of membrane as templates instead of filters for making nanowires is Possin and he used track-etched mica as template to synthesize Sn nanowires for superconducting studies in 1970 [55]. Recently, Martin [15], Wang *et al* [16] and Peng *et al* [17] have investigated the track-etched polycarbonate membrane as template to synthesize metallic nanowires by employing electrochemical deposition technique. Xu and Chen *et al* [56] synthesized CdS

semiconductor nanowires using anodized alumina membrane (AAM) as template. Subsequently, Mayer *et al* [57], Forrer *et al* [58] and Zhang *et al* [59] fabricated metallic nanowires based on electrodeposition technique in nanopore template of anodized alumina membrane (AAM).

1.2.1.1.1 Anodized Alumina Membrane (AAM)

Figure 1.1 is the SEM images of commercial Anopore® anodized alumina membrane bought from Whatman company which is one of the main AAM manufacturer [60]. The commercial anodized alumina membranes generally have high pore density, relatively precise pore structure and narrow pore size distribution *etc* characteristics, and they are usually made for filtration applications. The alumina membranes are made of high purity aluminum and manufactured electrochemically. They have hydrophilic properties and are compatible with most solvents and aqueous materials. These inorganic membranes manufactured by Whatman Company usually have 60μm thickness and 25-50% porosity.

(a)

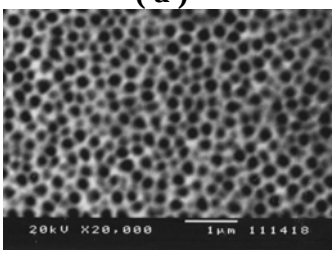

(b)

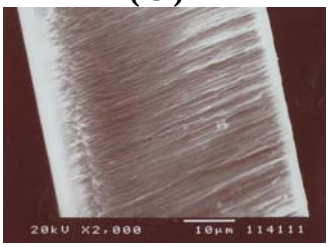

Figure 1.1 SEM images of Anopore® anodized alumina membrane, a) top view, ×20,000, b) cross-sectional view, ×2,000

The big drawback of these commercial AAMs is that they have some lateral crossover problems among vicinal individual pores, especially the area close to the two ends of pores, which make the subsequently fabricated nanowires difficulty to disperse and also affect magnetic properties of nanowire array due to the non-uniform interactions among vicinal individual nanowires. Another drawback is that these membranes usually have deformed pores instead of normally round shape (Figure 1a).

The fabrication of anodized alumina membrane in lab is a very intense and cumbersome job. The AAM template fabrication method was developed by Masuda in 1995[62], called two-step anodization procedure. The general procedures for making AAM are described below: First, high pure aluminum foil is vacuum annealed and the annealed aluminum foil then will be electropolished in a mixture solution of perchloric acid and ethanol with a certain ratio. The electropolished step will make the aluminum foil surface looks like a bright silver mirror. The following step after electropolishing is to employ the first anodization at a certain constant voltage. The whole anodization processing is performed in an oxalic acid solution. Then, the phosphoric acid and chromic acid mixture solution will be used to dissolve the just formed alumina layer during the first anodization. After removing the aluminum oxide layer, the initial hexagonal ordered honeycomb pore arrangement is achieved. The following second anodization applies the same parameters and conditions as in the first time set. After running the desired anodization time, the phosphoric acid and chromic acid mixture solution will be used again to remove the alumina layer. Eventually the more ordered and deep hexagonal honeycomb pores could be achieved with a certain thickness. The remaining pure aluminum layer at the bottom of sample can be dissolved by copper(II) chloride solution. For this two-step anodization

processing method, the anodization voltage controls the pore diameter size of AAM; the pore thickness is determined by the anodization time; the membrane porosity lies on the oxalic acid concentration. Figure 1.2 is the SEM images of the AAM fabricated by Masuda et al [62]. Comparing the Figure 1.2 to Figure 1.1, it is easy to see that the AAM made by Masuda *et al* had much better pore shape and uniformity than commercial one.

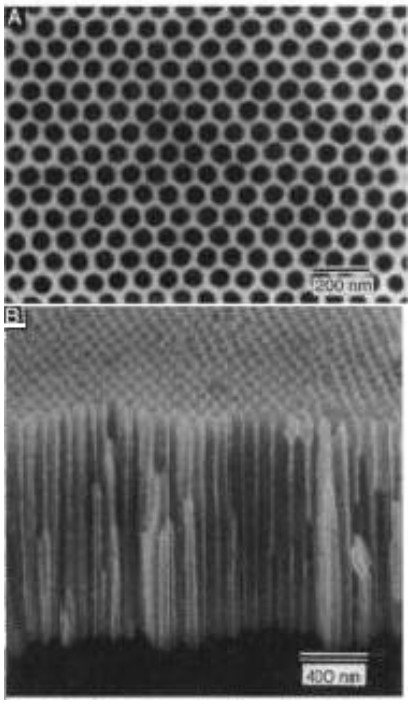

Figure 1.2 SEM images of anodized alumina membrane made by Masuda *et al*[62] , A) top view, B) cross-sectional view

1.2.1.1.2 Ion Track-Etched Membrane

The commonly used commercial ion track-etched membrane is polycarbonate membrane, which is initially also made for filters and cell culture [60]. Figure 1.3 is the SEM top view image of commercial Nuclepore® polycarbonate membrane manufactured by Whatman Company with 600nm pore size and 12μm thickness. The commercial polycarbonate membrane showed us that ion track-etched membrane has non-deformed

round pore shape, which is better than the commercial anodized alumina membrane (Figure 1.1a).

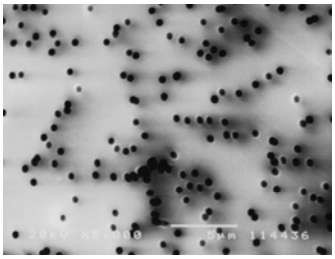

Figure 1.3 SEM top view image of Nuclepore® polycarbonate membrane with pore size 600nm, (× 5,000)

The usual drawbacks of the ion track-etched membranes are low porosity, bad pore distribution and tilted channels. From Figure 1.3, we can find that the pores are distributed randomly and some are overlapped partially among vicinal those. These characteristic drawbacks of ion track-etched membranes are determined by their fabrication method, which is inevitable. Briefly, the ion track-etched membrane fabrication procedures could be described as below [63]: An intact thin membrane film is exposed to a heavy ion source. The heavy ion beam will randomly bombard the membrane film, which will leave bombardment tracks inside membrane film with damaged polymer molecular structures. The chemical etching technique will be used to remove the bombardment tracks due to their damaged polymer molecular structures and keep the remaining area of the membrane intact. Therefore, the reason why ion track-etched membranes having lots of partially overlapped pores is the random ion bombardment. Besides, the tilted channels are contributed from the angler between the member surface and the flying path of heavy ions is not exact perpendicularity, which is caused by the unparallel flying path of ions. The low porosity could be overcome by increasing the ion bombardment time. However, with the increase of the ion

bombardment time, the chance to form partially overlapped pores will increase dramatically.

1.2.2 Electrodeposition Fabrication

Electrodeposition has been widely used in making thin films and coating for a long period [50,64]. The working mechanism is pretty simple, which involves the application of an electric current through a certain concentration electrolyte containing the desired metal ions to reduce the metal ions into metal on the cathode (or substrate). If electrodeposition employing on some non-conductive substrates, some pretreatments would be applied first on the surface of the non-conductive substrates, such as electroless chemical deposition or sputtering etc. The electrolyte could be aqueous solution of salts or fused salts. Electrolyte composition, applied potential, electrical current, electrolyte pH value and temperature are five main processing parameters of this electrodepostion technique.

In 1996, Martin [15] first employed this technique in synthesizing metallic nanowires using polycarbonate membrane as template. Subsequently, the electrochemical deposition has been used extensively in fabricating single metallic nanowries and multilayered metallic nanowires (superlattice) with controlled thickness for magnetic property studies [65]. For the electrodeposition process, a standard three-electrode plating cell is applied, which includes a working electrode, a counter electrode and a reference electrode. Usually the applied substrate will be served as the working electrode and several inert metals will be served as counter electrode and reference electrode, such as Pt wire. The standard Ag/AgCl is also the often-used reference electrode. The template-directed electrodeposition synthesis has been proved as the particularly high yield technique for

fabricating nanowires [66,67]. A single-bath technique is the commonly used approach to synthesize the single component metal nanowires. The electrobath only contains the desired single metal ions as electrolyte solution for deposition. For fabricating multilayered metallic nanowires (or superlattice), there are two approaches through the template-directed electrodeposition synthesis technique. The single-bath technique is widely used in most recent research work. The electrolyte solution is the mixture of two or more different metal ions. By controlling the applied potential and the concentration of the different metal ions, the reduction order of the desired metals could be arranged. One drawback of the single-bath technique is the co-deposition problem, which involves that there are two or more different metals could be reduced at the same time when applying a certain potential. However, adjusting the concentration of the different metal ions and choosing suitable applied potential could minimize this drawback. An alternative approach to synthesize the multilayered metallic nanowires is the dual-bath or multi-bath technique. The number of the components composing the multilayered metallic nanowires determines the number of the electrobath. Each electrobath only contains one single metal ion. The template substrate will move among different electrobaths to employ the electrodeposition. By employing this dual-bath or multi-bath technique, the co-deposition problem could be finally avoided, which can ensure each single segment in the multilayered metallic nanowires is one single pure metal we desired.

Chapter 2

Fabrication and Characterization of Metallic Nanowire Arrays

2.1 Introduction

Metallic nanowire arrays have recently attracted considerable attention due to their electrical, optical and magnetic properties and their potential application in high-density magnetic recording media and tunable microwave device [35,36,68,69]. The complicated and high-cost lithographic patterning fabrication technique for making metallic nanowire arrays is not suitable for large numbers of production and could not be applied extensively [70]. The template-directed electrochemical deposition technique has bee approved a good alternative approach in synthesizing metallic nanowire arrays and has been widely used in fabricating most metallic nanowire arrays with well-defined structure for magnetic property studies.

2.2 Experimental Section

2.2.1 Materials and Equipment

All chemicals were of reagent quality and were used as received. Dichloromethane (99.5%, EM science), acetone (99.7%, Mallinckrodt), ethyl alcohol (99.5%, Aldrich), and NaOH (98%, Sigma). The commercial gold (Orotemp 24 RTU, $KAu(CN)_2$, containing 8.2g/liter gold, pH ~ 8.0) and nickel (Nickel sulfamate-RTU, $Ni(H_2NSO_3)_2$, pH ~ 4.0) plating solutions were purchased from Technics, Inc.. Besides, the commercial copper (Cyanide) plating solution was obtained from Samson Technology Corp. The Anopore® anodized alumina membranes (AAMs) and Nuclepore® Track-etched polycarbonate

membranes were purchased from Whatman company. Besides, several alumina membranes were obtained from Professor Jin-Seung Jung research group (Department of Chemistry, Kangnung National University, South Korea). The Pd-Au and Ag sputtering target were purchased from Denton Vacuum Company. Silver paste and 3M Scotch Super Strength glue was obtained from Ted Pella, Inc. and VWR Company respectively.

The Denton Desk II cold sputter/etch unit carried out magnetron sputtering deposition. Princeton Applied Research VMP2 Multichannel Potentiostat Systems was used to perform electrochemical deposition. JEOL JSM 5410 Scanning Electron Microscope (SEM) took scanning electron micrographs.

2.2.2 Fabrication of Metallic Nanowire Arrays Using Anodized Alumina Membrane (AAM) as Template

The metallic nanowire arrays were fabricated by electrochemical deposition into the channels of anodized alumina membrane (AAM) template using a standard three-electrode plating cell containing desired metal ions [71]. The specific fabrication procedures are showed in Figure 2.1 and will be discussed in detail below.

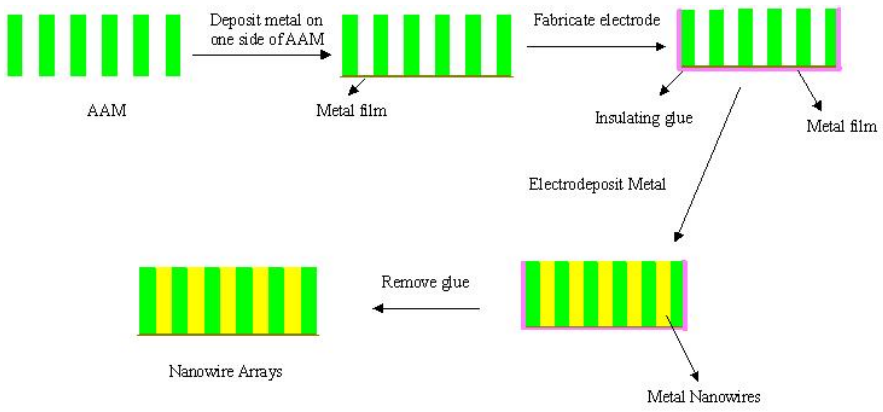

Figure 2.1 Schematics of metallic nanowire array fabrication

2.2.2.1 Conversion of Anodized Alumina Membrane Template into Electrode

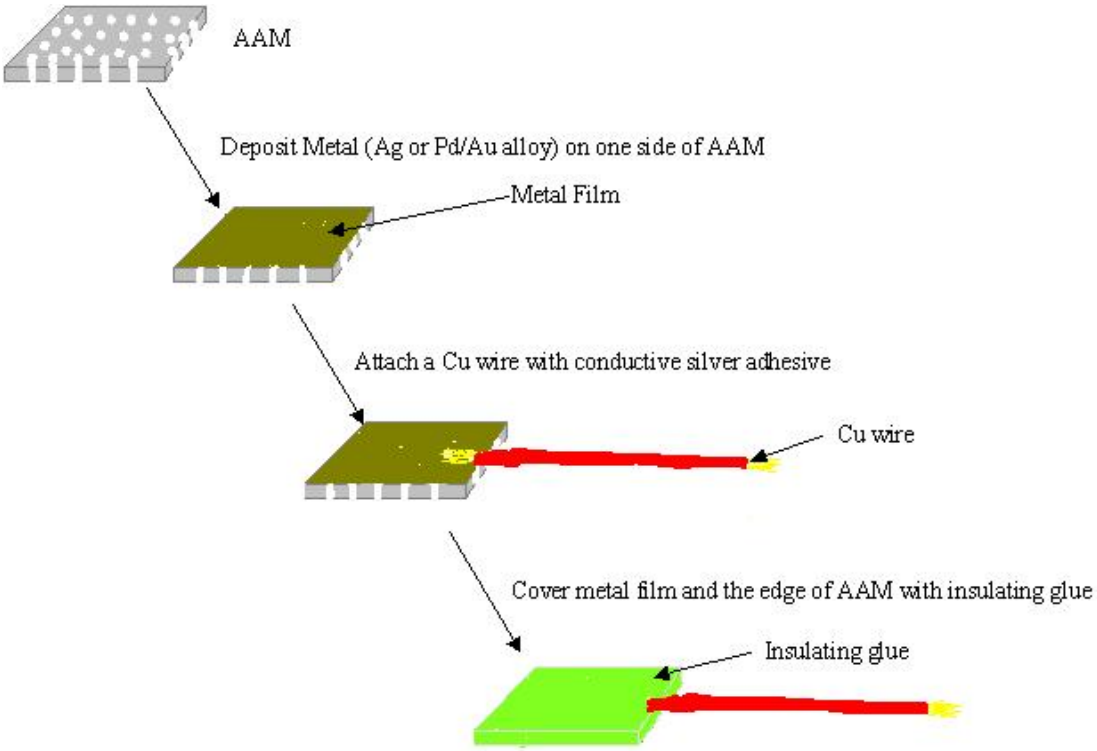

Figure 2.2 Schematics of AAM electrode fabrication

Figure 2.3 Denton Desk II cold sputter/etch unit

The AAM electrode fabrication is the initial step for the whole template-directed electrochemical deposition process. Figure 2.2 is the fabrication schematics of conversion from a piece of anodized alumina membrane (AAM) template to a working electrode. The AAM is a fragile and insulating inorganic material and we need to convert this insulating material to be electrically conductive and served as an electrode. The Denton Desk II cold sputter/etch unit (Figure 2.3) was utilized to deposit a thin metal film on one side of the AAM membrane. The Denton Desk II cold sputter/etch unit can work with different metal targets, such as Au, Ag, Cu, Pd and Pd/Au alloy. In our research group, the Ag and Pd/Au alloy targets were the usual sputtering metals for different purposes. These two different metal targets have advantages and disadvantages respectively. If our objective is to make freestanding nanowires, we generally use Ag as the sputtering metal because it is easy for us to remove it from AAM template during the post-treatment process. Usually we use nitric acid to dissolve or sandpaper to polish. However, if the object is to make nanowire arrays, usually the sputtering metal is not necessary to remove after finishing electrodepostion. Therefore, the Pd/Au alloy as sputtering target is a good choice. One advantage with Pd/Au alloy is its good stability in the air. If we use Ag as the sputter metal, we know metal Ag could be oxidized slowly to form a thin AgO film, which will affect the subsequent electrochemical deposition performance and decrease its deposition efficiency. Besides, another purpose of sputtering metal on one side of AAM is to seal one end of all membrane pores. Otherwise, the following electrochemical deposition processing to deposit nanowires into AAM channels will be difficult to realize. For this Denton Desk II sputter system, the deposition speed depends on the parameters we set. Generally, we use 45 milliamps as the sputter intension and the

deposition speed is 0.33 nm/second. The different substrate surface uniformity and target metal composition also slightly affect the deposition speed and efficiency.

After sputtering metal with a certain thickness (200-300nm) on one side of a piece of AAM, the following step is to attach a 15-20cm long conductive wire, the commonly used is copper wire because of its low-cost and having good electric conductivity, on the metal film side of AAM using conductive silver paste. The bond strength between conductive wire and metal film of AAM mainly depends on the concentration of conductive silver paste, but the most concentrated is not the best because it is difficult for the most concentrated paste to spread out to make sufficient contact between conductive wire and the sputtered metal film, which will also decrease the bond strength. The concentration of silver paste can be adjusted by addition of acetone. Besides, there is another point we need to be aware of. The silver paste has to be solidified in the air for sufficient time, which make the attachment much more stronger. Otherwise, the conductive wire could be peeled off on the metal film of AAM due to the dissolution of silver paste when it is immersed in the electroplating solution for a certain long period during electrochemical deposition processing.

The last step of making an AAM electrode is the seal using insulating polymer glue (3M Scotch Super Strength glue). The purpose of sealing with insulating polymer glue is to direct the metal reduced from electrolyte solution to fill into the desired area, the inside of AAM channels. Otherwise, the most metal could be deposited on the undesired area, the surface of sputtered metal film, which will not only decrease the electrochemical deposition efficiency, but also decrease the sample quality. Besides, the around edges of AAM also need to be covered by the insulating glue to avoid the unnecessary deposition.

2.2.2.2 Electrochemical Deposition in the Channels of AAM Template

Electrochemical deposition was performed on a Princeton Applied Research VMP2 Multichannel Potentiostat Systems through a standard three-electrode plating cell (Figure 2.4) with a constant current method. In this standard three-electrode plating cell, the fabricated AAM template was served as a working electrode, and the counter electrode and reference electrode were two high pure platinum wires. In order to precisely control the working potential, Ag/AgCl standard electrode were sometimes used as a reference one. It is unnecessary to use Ag/AgCl standard electrode as the reference electrode if the constant electric current method was performed because the electric current density and electrodeposition time are the only two controlling parameters in tailoring the nanowire products under constant electric current condition. In this Princeton Applied Research VMP2 Multichannel Potentiostat Systems, the applied software includes a chronopotentiometry mode, which could allow us to choose a certain electric current value to run the electrochemical deposition experiment. The working electrode area can be calculated based on the AAM template size. Therefore, the electric current density of the working electrode can be calculated from above data. Once the current density is fixed, the amount of the reduced metal from electroplating solution only depends on the experiment time. Based on the previous studies in our research group, the current density was usually set to 0.5 mA/cm^2 or smaller. The commonly used current density value is 0.1 mA/cm^2 . Under this parameter, the rough nanowire growing speed of Au and Ni is 300nm/hour and 100 nm/hour respectively. Theoretically, the nanowire growing speed also could be calculated based on coulomb value. However, the theoretical calculation needs to know the electrochemical deposition efficiency because the electric current

through the working electrode couldn't be used with 100% to perform reductive reaction to reduce metal ion to metal.

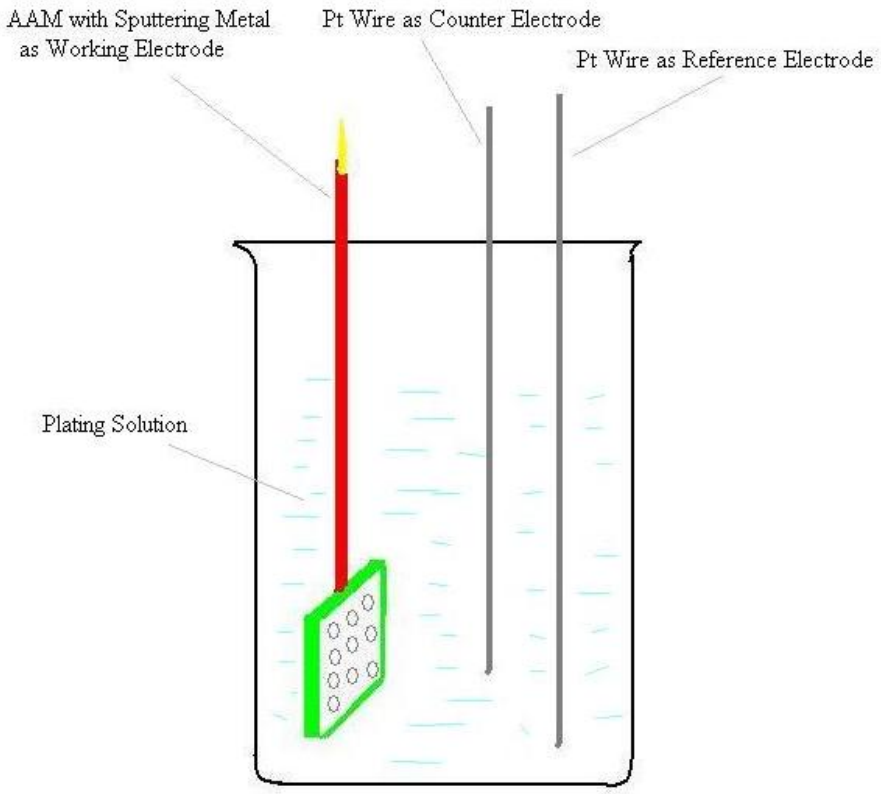

Figure 2.4 Schematics of a Standard Three-Electrode Plating Cell for Performing Electrochemical Deposition Using AAM as Template

2.2.2.3 Sample Post-Treatments

The specific post-treatments depend on the different research goals. For this research project, we want to get the metallic nanowire arrays with AAM template remaining in order to investigate their magnetic properties. Therefore, the post-treatment processing of sample after finishing electrodeposition is relatively simple and we just need to remove the insulating polymer glue and the attached metal wire. The dichloromethane (99.5%, EM science) or acetone (99.7%, Mallinckrodt) is the commonly used solvent to

dissolve insulating polymer glue. In the meantime, the silver paste also will be softening in these organic solvents and the metal wire could be detached easily. For this process, the troublesome thing is that the insulating polymer glue cannot be dissolved away as quickly as we expect in either one of two organic solvents. If the polymer glue cannot be removed totally, the softening polymer glue could wrap up the nanowires, which will make the following sample characterization using scanning electron microscope (SEM) to be extremely difficult because the polymer glue is electrically non-conducting material, which could make the SEM image look fuzzy. This fuzzy phenomenon is due to the electrons accumulation on the non-conducting surface of sample, which makes the focus of SEM become dramatically difficult. Usually, the soak time of sample in the organic solvent for removing polymer glue is up to several days. Moreover, the organic solvent needs to be changed very often (every 10 to 12 hours), which could allow the refreshing organic solvent to speed up the dissolution process.

After dissolving the polymer glue and removing metal wire, we used sandpaper to slightly polish the metal film side of AAM temple in order to get rid of solidified silver paste and sputtered metal film. Finally the nanowire arrays embedded in AAM template were obtained. Besides, in order to prevent several deposited metal (such as nickel, copper etc.) from oxidizing, the samples were kept in ethyl alcohol solution (99.5%, Aldrich) to avoid contacting air because the oxidized metal nanowire arrays would affect their magnetic property measurements.

Moreover, if we have to get freestanding nanowires for characterization on SEM, some extra treatments need to be done. The sputtered metal can be removed using sandpaper polish. If the sputtered metal is silver, we also can use nitric acid to dissolve.

But this process needs to be extremely careful because the strong acid also could dissolve several types of metal nanowires (such as nickel, copper and cobalt etc.) although they are embedded in the channels of AAM template. The anodized alumina membrane can be dissolved in strong base solution (such as 2M NaOH or KOH). The warm sodium hydroxide or potassium hydroxide solution could speed up the dissolution of AAM template. After dissolving the AAM template, the freestanding metal nanowires would precipitate at the bottom of container while treating with centrifuge. After washing sample with deionic water for several times, the nanowires were kept in 99.5% ethyl alcohol solution and ready for SEM observation.

2.2.3 Fabrication of Metallic Nanowire Arrays Using Ion Track-etched Polycarbonate Membrane as Template

The fabrication of metallic nanowire arrays using ion track-etched polycarbonate membrane as template is slightly different with that using AAM as template. The reason is that the polycarbonate membrane is very soft organic material and it is not like AAM that is hard inorganic material. Therefore, the way for making AAM working electrode depicted above could not work out for fabricating soft polycarbonate membrane electrode. Several additional techniques need to be applied to modify the above AAM electrode fabrication procedures to make it suitable for soft polycarbonate membrane. An Open-Face Delrin* Filter Holder (Figure 2.5) was utilized in making the polycarbonate membrane electrode. Figure 2.6 is the Nuclepore® Track-etched polycarbonate membranes (25mm, Whatman). In life science research lab, this ion track-etched membrane combined with the filter holder is generally served as a filter. In order to

make polycarbonate membrane electrode, a few of modifications was made on this filter holder, which is showed in the Figure 2.7.

Figure 2.5 Open-Face Delrin* Filter Holder (25mm, Pall* Life Sciences)

Figure 2.6 Nuclepore® Track-etched polycarbonate membrane (25mm, Whatman)

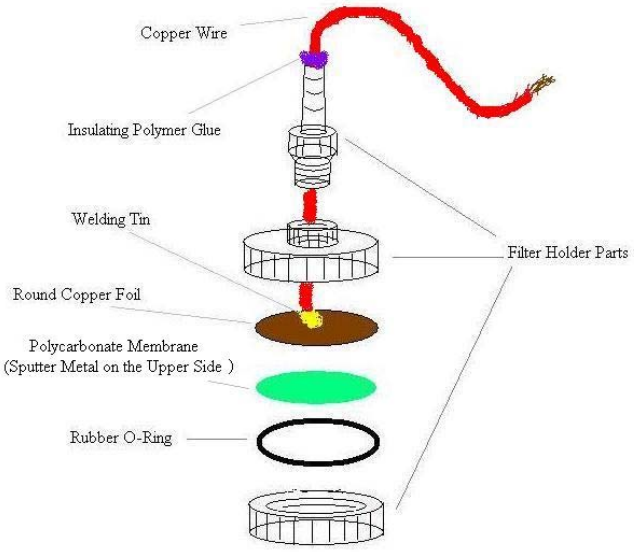

Figure 2.7 Assembly schematics of polycarbonate membrane electrode fabrication

For this modification, there was no insulating polymer glue been used directly on the sputtered metal surface of polycarbonate membrane. The insulating polymer glue was

used indirectly in this fabrication to prevent plating solution leaking from filter hold pipeline. Moreover, the conducting wire is not directly bond to sputtered metal side of polycarbonate membrane, but wedding to a thin conducting copper foil. The advantage of this modification is to decrease the workload of post-treatment of sample because the sample membrane is easily to be peeled off and there is no polymer glue need to be dissolved or a piece of conducting wire have to be removed from membrane template. Based on the schematics of a standard three-electrode plating cell showed in Figure 2.4, we just need use this polycarbonate membrane electrode to substitute the AAM electrode and we are ready to make metallic nanowires in the channels of soft track-etched polycarbonate membrane (Figure 2.8).

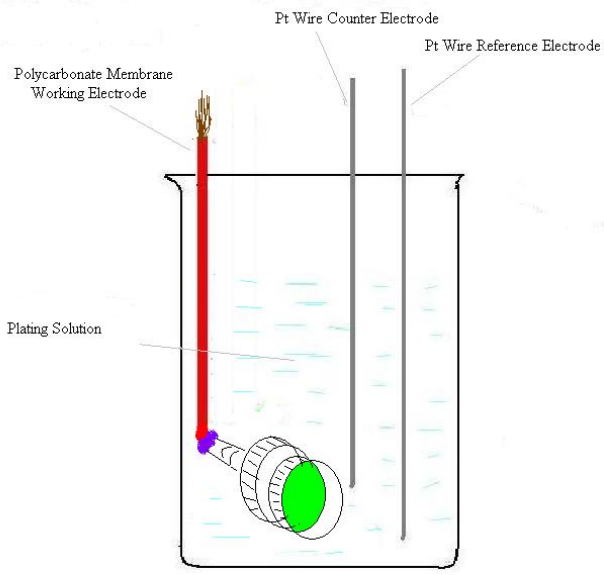

Figure 2.8 Schematics of a standard three-electrode plating cell for performing electrochemical deposition using polycarbonate membrane as template

Besides, the post-treatment was relatively simpler comparing to the AAM template sample. There is no troublesome insulating polymer glue to be dissolved. In order to obtain freestanding nanowires for SEM observation, the sputtered metal film on the

membrane can be polished away using sandpaper. The polycarbonate membrane itself was much easier to be dissolved in dichloromethane organic solution.

2.2.4 Scanning Electron Microscope (SEM) Characterization

JEOL JSM 5410 Scanning electron microscopy (SEM) with energy dispersive X-ray spectroscopy (EDX) analysis performed sample characterization. The nanowire ethanol solution was dropped on the conductive carbon tape that is bond to a SEM sample mount. After the evaporation of ethanol, the sample mount was loaded into SEM sample chamber for observation. If the observed sample is non-conducting material, such as polycarbonate membrane or anodized alumina membrane, the Denton Desk II cold sputter system was used to deposit a very thin layer of metal, Au or Pd/Au etc., on the surface of sample to make sample surface become electrical conductive before SEM observation.

2.3 Results and Discussion

2.3.1 SEM Images of Single Metal Nanowires

The template-directed electrochemical deposition method can fabricate well-defined single metal nanowries. The electrochemical deposition begin to reduce the metal cation of the plating solution at the bottom of inside channels of template because the sputtered metal can be served as cathode and then grow toward to the open side of membrane channels.

2.3.1.1 Electrochemical Fabrication Using AAM as Template

Figures 2.9a,b,c,d,e,f,g shows several cross-sectional view SEM images of nickel nanowire arrays after dissolving AAM template using 2M potassium hydroxide solution.

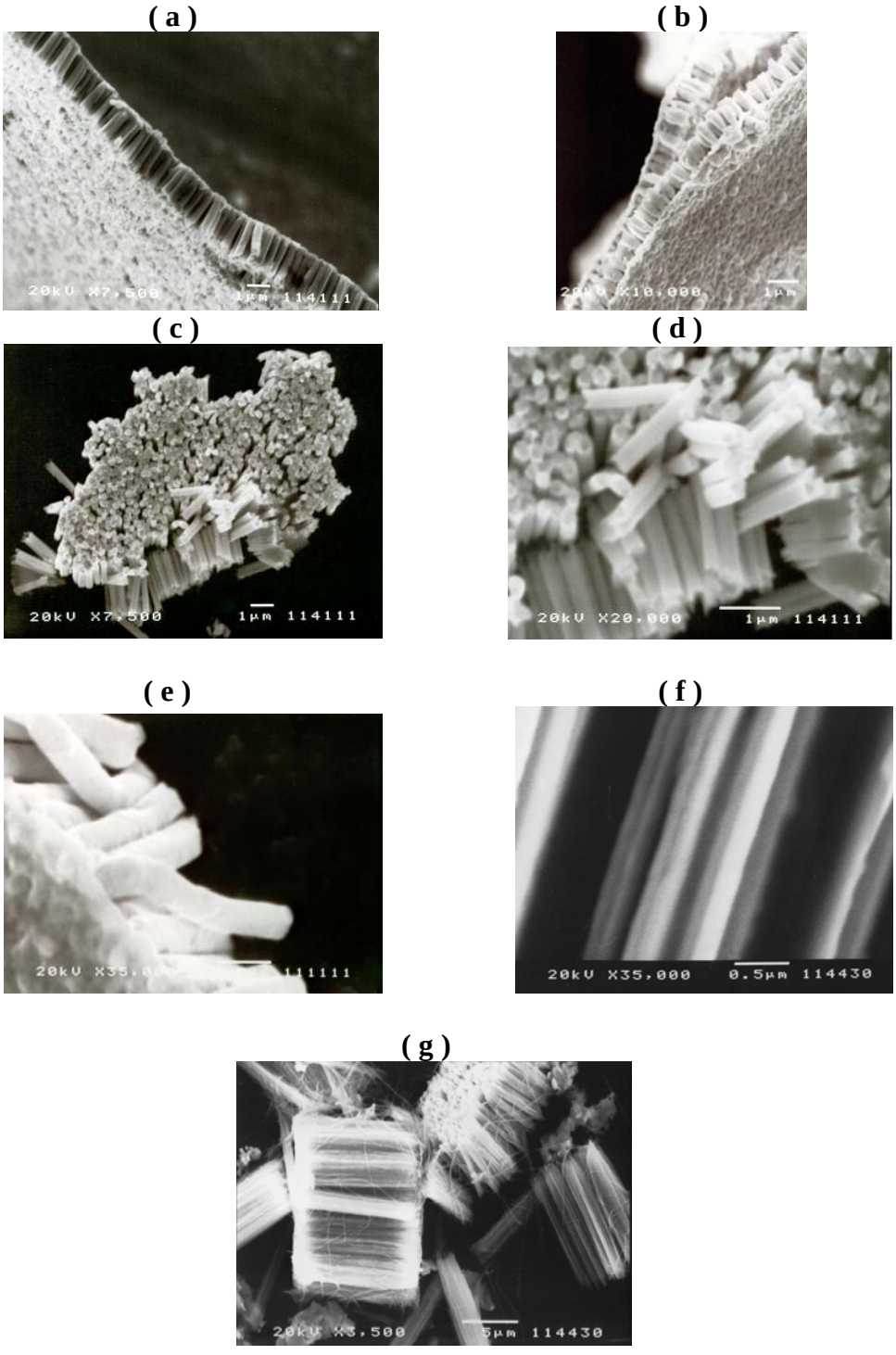

Figure 2.9 SEM images of Ni nanowire arrays

a) Ø=400nm, ×7,500, b) Ø=500nm, ×10,000, c) Ø=300nm, ×7,500, d) Ø=300nm, ×20,000, e) Ø=400nm, ×35,000, f) Ø=60nm, ×35,000, g) Ø=60nm, ×3,500

Hereinto, the template used for making nanowires in the Figures 2.9a,b,c,d,and e were the commercial AAM obtained from Whatman Company. In the Figure 2.9f,g, we used lab-made AAM as temple obtained from Professor Jin-Seung Jung research group (Department of Chemistry, Kangnung National University, South Korea) to make these Ni nanowire arrays. In Figures 2.9a,b,e, all the nickel nanowires stand on the substrate that is Pd/Au alloy film we sputtered using Denton Desk II Cold Sputter/Etch Unit. Besides, we mentioned before that the big drawback of the commercial AAMs is that they have some lateral crossover problems among vicinal individual pores, especially the area close to the two ends of pores, which make the subsequently fabricated nanowires difficulty to disperse. From Figures 2.9c, d, we can clearly see that nanowires made from these types of commercial AAMs still could form a bunch of arrays even if we removed the metal film substrate using sandpaper polish technique. Besides, from Figure 2.9e we can find that not all commercial AAM channels were straight enough. Moreover, the nanowire cylinder surface is not smooth enough and there are some small bumps existed. Relatively, the AAM obtained from Jin-Seung Jung research group are much better than the commercial AAM.

Figures 2.10a,b are two top view SEM images of nickel nanowire arrays. We can find that the transection shapes of nanowires are not typically round, which is decided by the channel shapes of commercial AAM because they are not round enough (Figure 1.1a). Meanwhile, there are some defects (nanowires missing) found in the images. There are two possible reasons that could cause these defects. One is that the previous sputter metal didn’t seal the end of that AAM channel well. Therefore, the nickel ions could not be

reduced and deposited into that channel. Another possible reason is that nanowire was broken due to applied forces during post-treatment processes, such as centrifuging force.

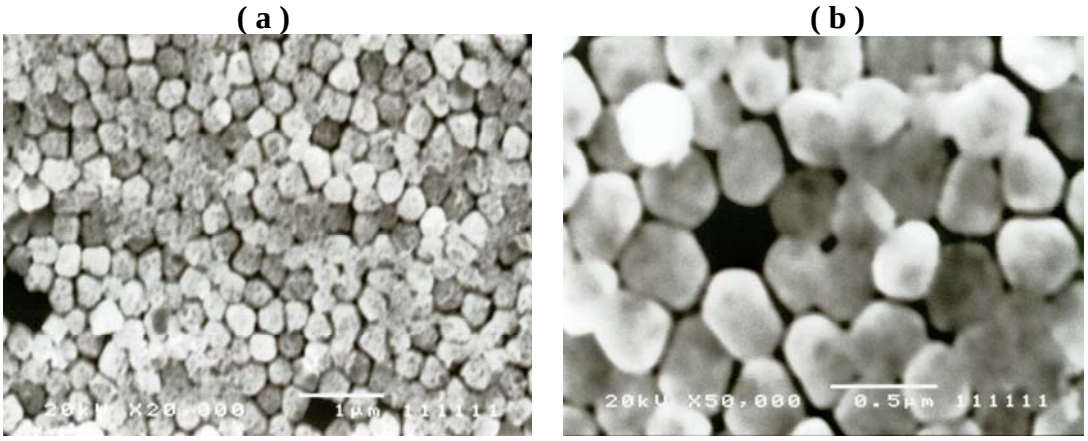

Figure 2.10 Top view SEM images of Ni nanowire arrays
a) Ø=400nm, ×20,000, b) Ø=400nm, ×50,000

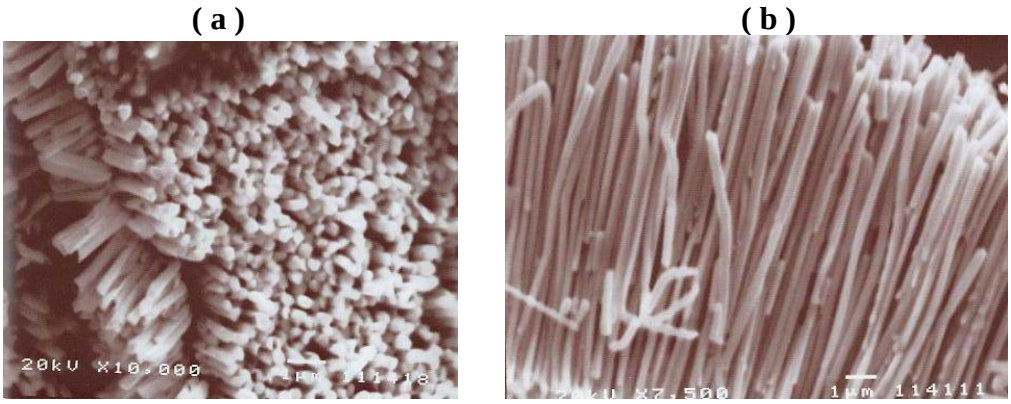

Figure 2.11 SEM images of Au nanowire arrays
a) Ø=300nm, ×10,000, b) Ø=300nm, ×7,500

Figures 2.11a,b are SEM images of gold nanowire arrays after dissolving AAM template using 2M potassium hydroxide solution. Figure 2.12 is the top view SEM image of gold nanowire arrays. After polishing off sputtered Pd/Au alloy film, we got freestanding gold nanowires (Figures 2.13a,b,c,d). From Figure 2.13a, we can clearly see

that the zigzag shape of the nanowire cylinder body due to the roughness inside some individual channels of commercial AAM templates.

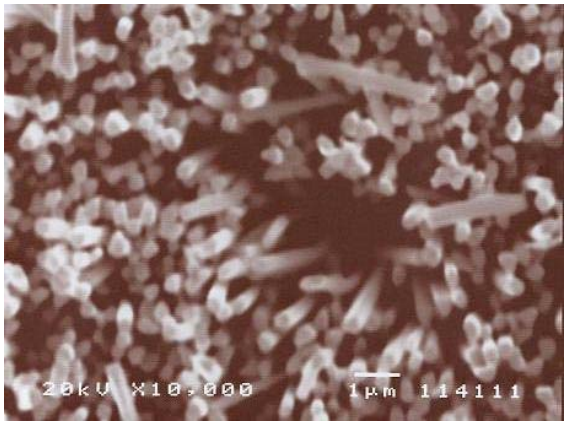

Figure 2.12 Top view SEM image of Au nanowire arrays (Ø=300nm, ×10,000)

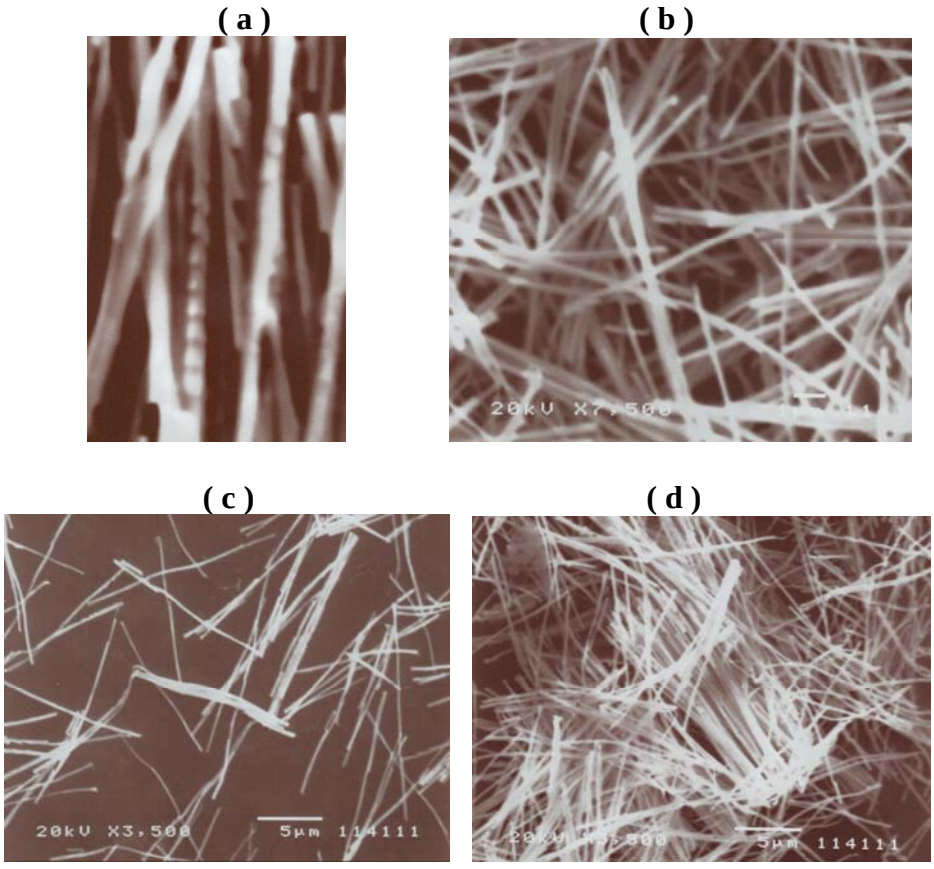

Figure 2.13 SEM images of freestanding Au nanowire a) Ø=300nm, ×20,000, b) Ø=300nm, ×7,500 c) Ø=300nm, ×3,500, b) Ø=300nm, ×3,500

Interestingly, there was once that the electrodeposition was run overtime. After nickel metal finish filling the entire channels of AAM template, it started to deposit on the surface of the AAM template. We can clearly see this phenomenon from Figure 2.14a because the sample formed two obvious layers. Especially, the top view SEM images showed us the interestingly ‘unique’ nanostructures (Figure 2.14b). Moreover, the Figure 2.14b showed us that the special nanostructures were formed through layer by layer.

(a) **(b)**

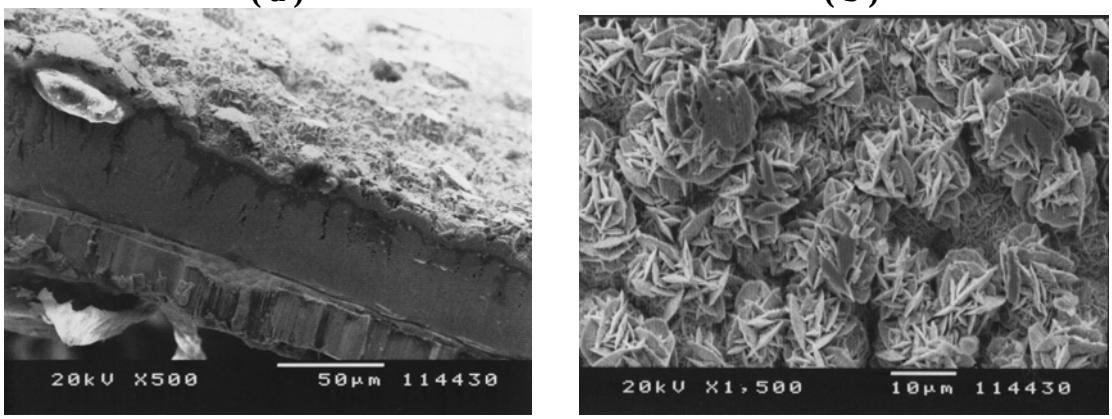

Figure 2.14 SEM images of the ‘unique’ nanostructures a) ×500 , b) ×1,500

2.3.1.2 Electrodeposition Fabrication Using Track-Etched Polycarbonate Membrane as Template

Nickel nanowire arrays were electrochemically fabricated into cylindric channels of commercial ion track-etched polycarbonate membranes. Figure 2.15 are the SEM images of Ni nanowire arrays standing on the sputtered Pd/Au alloy after dissolving polycarbonate membrane template using dichloromethane. Comparing to nanowires electrochemically synthesized using commercial AAM as template, the nanowires fabricated electrochemically based on track-etched polycarbonate membranes have much

better diameter uniformity and smooth surface. The drawback is that the nanowire density is low (membrane pore density around $10^9/cm^2$) and the distribution is not uniform, which could affect the subsequent magnetic property measurements due to the different interactions among vicinal individual nanowires.

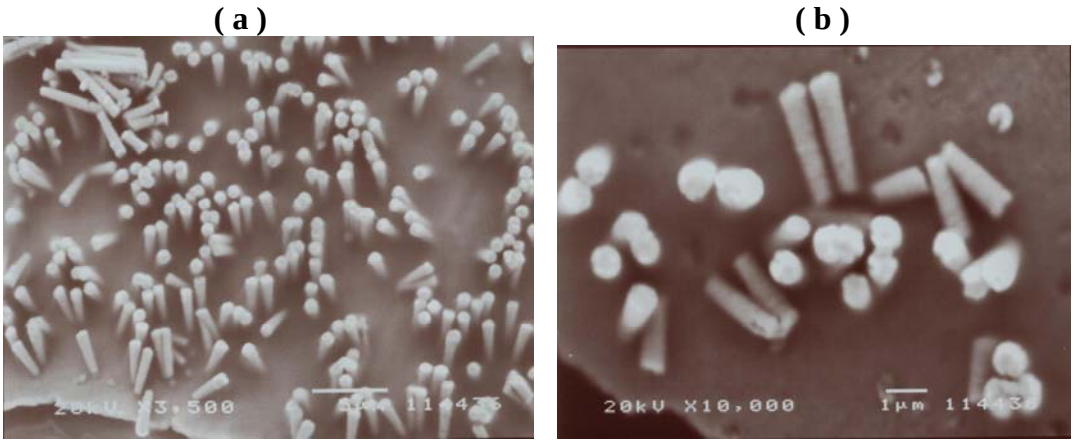

Figure 2.15 SEM images of Ni nanowire arrays after dissolving polycarbonate membrane template a) Ø=600nm, ×3,500, b) Ø=600nm, ×10,000

2.3.2 SEM Images of Ni/Au Multisegmental Nanowires

Ni/Au multisegmental nanowires were electrochemically synthesized into cylindric channels of AAM template with different pore size using dual-bath technique to avoid the co-deposition problem that could be caused by single-bath technique. Figure 2.17 and 2.18 are SEM images of Ni/Au multisegmental nanowire arrays fabricated using AAMs as template. In all pictures, the dark segments are nickel metal and the light segments are gold metal. The length of the metal segments was controlled by the electrodepostion time. From Figures 2.17a,b,c, we can find that there are some detached gold segments, which was possibly caused by the centrifuge force used during the post-treatments period. Besides, when we move the working electrode from one electrolyte bath to another electrolyte bath, the electrode should be soaked and washed completely in deionic water

for sufficient time. Otherwise, the previous electrolyte solution would remain the inside of template channels, which could contaminate the next electrolyte solution and make the interface between the vicinal two different composition segments blur and unparallel (see Figure 2.18).

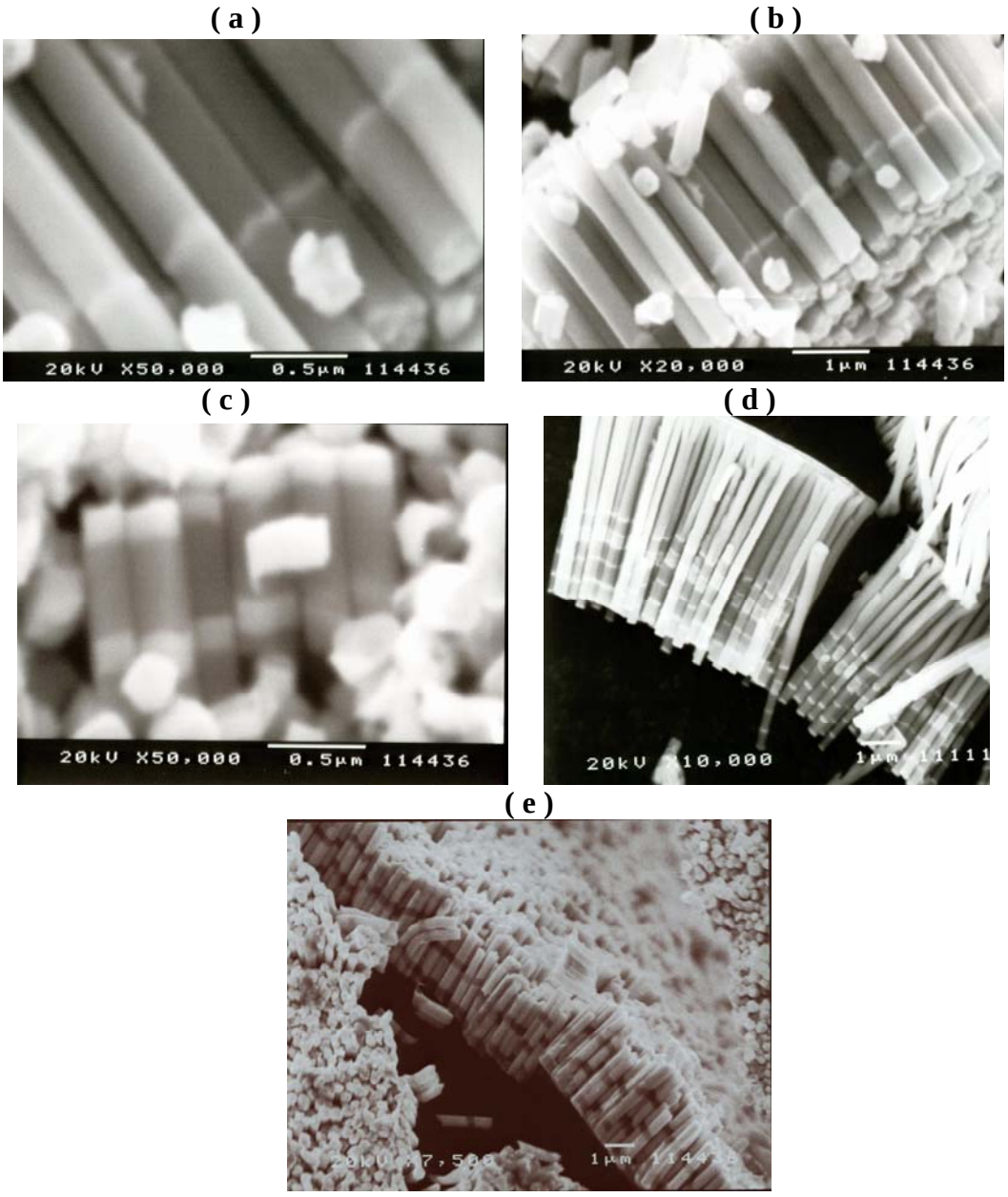

Figure 2.17 SEM images of Ni/Au multisegmental nanowire arrays a) Ø=300nm, ×50,000, b) Ø=300nm, ×20,000, c) Ø=200nm, ×50,000, d) Ø=400nm, ×10,000, e) Ø=500nm, ×7,500

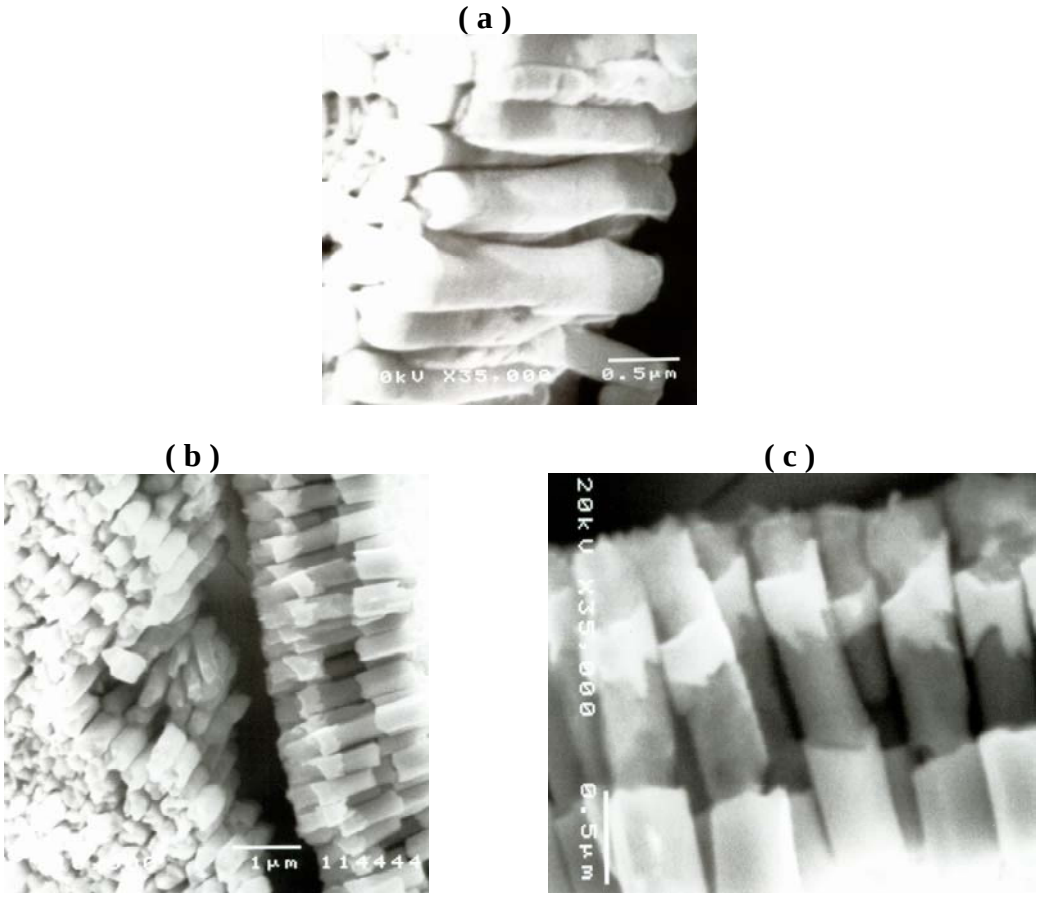

Figure 2.18 SEM images of Ni/Au multisegmental nanowire arrays a) Ø=500nm, ×7,500, b) Ø=400nm, ×20,000, c) Ø=400nm, ×35,000

2.3.3 SEM Observation after Modification of Multisegmental Nanowires

Ni/Au multisegmental nanowires could be modified using diluted HCl solution to form some other interesting structures showed in Figure 2.19 because the diluted HCl solution only can dissolve Ni metal and keep Au metal intact. Moreover, if the sample was soaked in diluted HCl solution for a very short time, there only the partial nickel metal have been dissolved and we could get such type of nanostructures as showed in Figure 2.19 a, b and c. If the soak time is long enough, then the nickel segments were dissolved completely and just left gold segments, which could let us obtain gold nanodisks showed in Figure 2.19d.

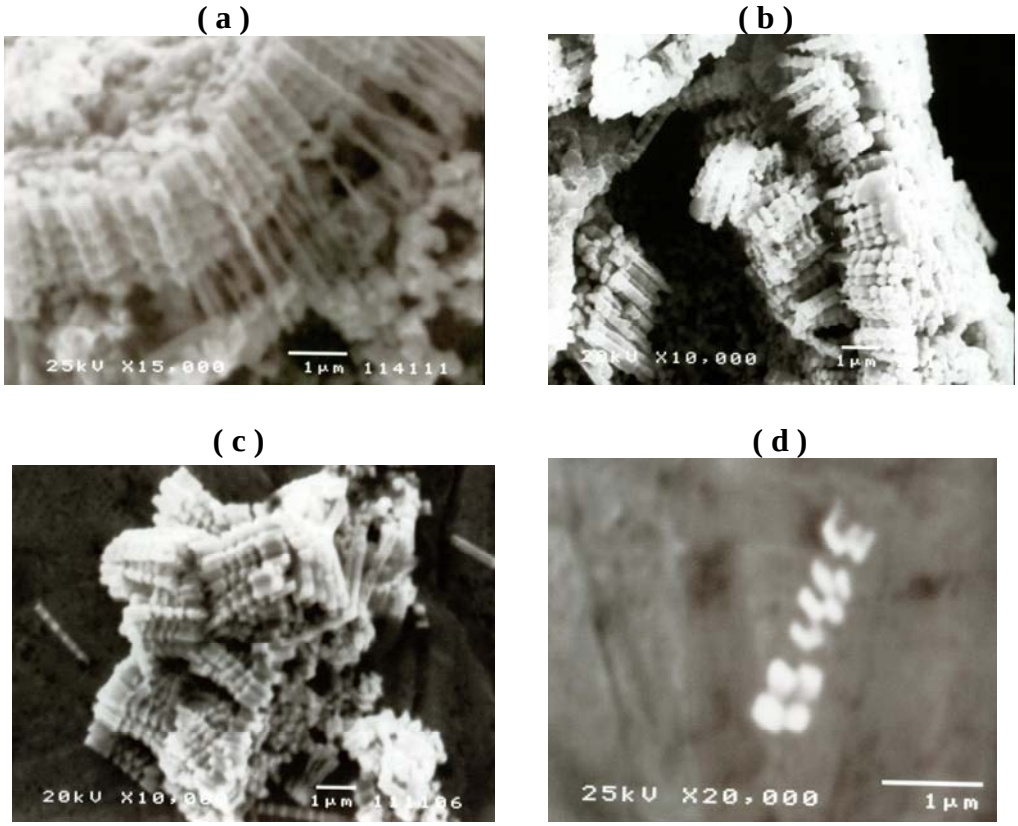

Figure 2.19 SEM images of modified multisegmental nanowires
a) Ø=300nm, ×15,000, b, c) Ø=400nm, ×10,000, d) Ø=300nm, ×20,000

2.4 Conclusions

The template-directed electrochemical deposition technique has been approved a good alternative approach in synthesizing metallic nanowire arrays and has been widely used in fabricating most metallic nanowire arrays with well-defined structure. The specific electrode making and electrochemical deposition procedures have been described in detail. Under constant electric current condition, the electric current density and electrodeposition time are the two controlling parameters in tailoring the nanowire products. The anodized alumina membrane (AAM) and ion track-etched polymer membrane are the most commonly used as fabrication templates. The dual-bath technique

was applied in synthesis of multisegmental nanowire arrays to avoid co-deposition problems caused by the single-bath technique. Several interesting nanostructures was obtained after modification of Ni/Au multisegmental nanowires using diluted HCl solution. The scanning electron microscopy (SEM) performed all sample characterization.

Chapter 3

Magnetic Property Investigation of Metallic Nanowire Arrays

3.1 Introduction

Metallic nanowire arrays synthesized by template-directed electrochemical deposition method have recently attracted considerable attention due to their potential applications in high-density magnetic recording media and tunable microwave device [35,36,68,69]. Vibrating sample magnetometer (VSM) and ferromagnetic resonance (FMR) techniques are two useful tools in investigating the magnetic properties of these metallic nanowire arrays. Vibrating Sample Magnetometer can allow us to easily get magnetization hysteresis loops at room temperature, which could provide us coercivity and remanence *etc* static magnetic properties about the tested samples. The ferromagnetic resonance (FMR) technique is a good tool in studying the dipolar interactions between the individual nanowires *etc* dynamic magnetic properties of metallic nanowire array system [72].

3.2 Experimental Section

3.2.1 Materials and Equipment

All Chemicals, materials and equipments unless otherwise stated were the same as those shown in chapter 2. Magnetic measurements were performed on a Lakeshore® 7307 Vibrating Sample Magnetometer (VSM) at room temperature. Ferromagnetic resonance spectra were recorded on a Bruker® EMX 102 Ferromagnetic Resonance (FMR) and Electron Paramagnetic Resonance (EPR) Spectrometer System using X-band (9.8 GHz) at room temperature.

3.2.2 Specimens of Ni Nanowrie Arrays and Ni/Cu Superlattice Nanowire Arrays

The specimens for the vibrating sample magnetometer (VSM) and Ferromagnetic Resonance (FMR) Measurements were Ni nanowire arrays and Ni/Cu superlattice nanowire arrays fabricated by electrodeposition using lab-made anodized alumina membrane (AAM) obtained from Professor Jin-Seung Jung research group (Department of Chemistry, Kangnung National University, South Korea). These AAM templates had a nominal radius of 60nm. By controlling the different electrodeposition time, we got Ni nanowires arrays with different lengths of 150nm, 300nm, 600nm and 1200nm. The dual-bath technique was employed in preparation of Ni/Cu superlattice nanowire arrays that contains four Ni segments of different length and three copper segments of same length with the structure Ni(150nm) – Cu(150nm) – Ni(300nm) – Cu(150nm) – Ni(600nm) – Cu(150nm) – Ni(1200nm).

3.2.3 Vibrating Sample Magnetometer (VSM) Measurements

The hysteresis M(H) loops data of series of metallic nanowire arrays were recorded on a Lakeshore® 7307 Vibrating Sample Magnetometer (VSM) at ambient temperature. A piece of nanowire array embedded in AAM or polycarbonate membrane was loaded on the specimen mount. The experimental data were recorded with the change of angle between the applied field and the nanowire axis.

3.2.4 Ferromagnetic Resonance (FMR) Measurements

A Bruker® EMX 10/12 Paramagnetic Resonance (EPR) Spectrometer System recorded the ferromagnetic resonance data of series of metallic nanowire arrays at ambient temperature. A piece of nanowire array embedded in AAM or polycarbonate

membrane was loaded on the specimen mount. The microwave absorption spectra were recorded using X-band (9.8 GHz) with the change of angle between the applied field and the nanowire axis.

3.3 Results and Discussion

3.3.1 VSM Spectra

The hysteresis loops of Ni nanowire arrays and Ni/Cu superlattice nanowire arrays are showed in Figure 3.1. These hysteresis loops were obtained with the external field applied parallel and perpendicular to the wire axis. The VSM measurement data in Figure 3.1 showed us that the easy axis is parallel to the nanowire axis direction, which could be explained from the major contribution of the shape anisotropy for nanowire arrays because they have large aspect ratio. Therefore, we can expect that the coercivity of the nanowire arrays for an external applied field parallel to the nanowire axis is larger than that for an applied field perpendicular to the nanowire axis. Besides, the hysteresis loops of Figure 3.1 also showed us that the saturation field for an external applied field parallel to the nanowire axis is smaller than that for an external applied field perpendicular to the nanowire axis, which also indicates that all nanowire arrays have obvious magnetic anisotropy along the nanowire axis direction. Moreover, the hysteresis loops of Ni nanowire arrays and Ni/Cu superlattice nanowire arrays in Figure 3.1 also shows that the remanent magnetization (Mr) for an external applied field parallel to the nanowire axis is larger than that for an external applied field perpendicular to the nanowire axis because the magnetic easy axis is aligned with the nanowire axis direction. Theoretically, if the magnetic easy axis or the axis of anisotropy is perfectly parallel to the external applied

field, the remanent magnetization (Mr) should be equal to the saturation magnetization (Ms); and if the magnetic easy axis or the axis of anisotropy is perfectly perpendicular to the external applied field, then the remanent magnetization (Mr) would be close to zero.

(a)

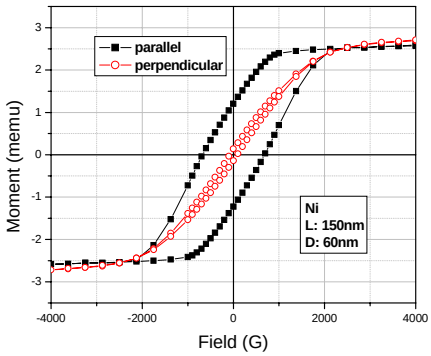

(b)

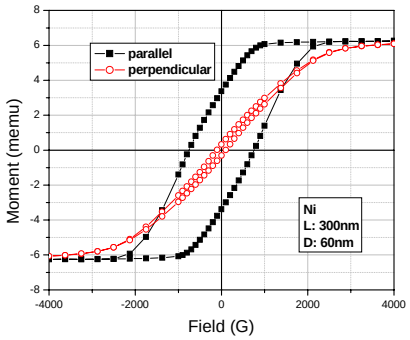

(c)

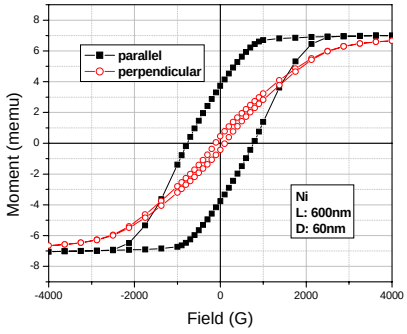

(d)

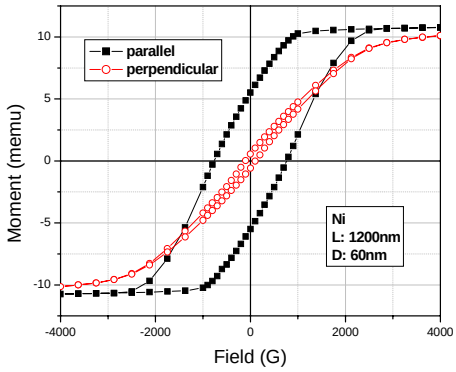

(e)

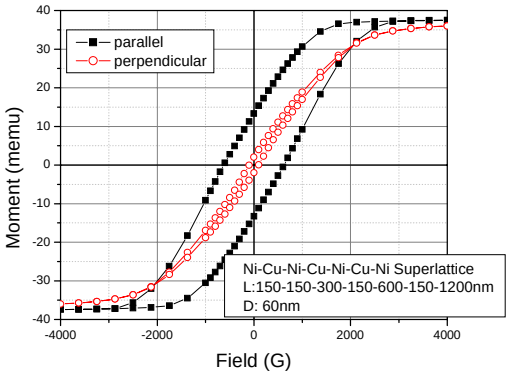

Figure 3.1 The hysteresis M(H) loops data of Ni nanowire arrays and Ni/Cu superlattice nanowire arrays measured with external field parallel and perpendicular to the wire axis

3.3.2 FMR Spectra

The sequence of FMR spectra at X-band (9.8Hz) recorded as function of the angle between the applied external field and the nanowire axis is showed in Figure 3.2. The sequence of FMR spectra of all single Ni nanowire arrays with different lengths (Figure 3.2 a, b, c, and d) showed us that the resonance field of the absorption peak increased by changing the angle between the applied external field and the nanowire axis from parallel (0°) to perpendicular (90°) because the wire axis is the effective magnetic easy axis.

However, the sequence of FMR spectra of Ni/Cu superlattice nanowire arrays in Figure 3.2e didn't show the same phenomenon as the single Ni nanowire arrays. When the applied external field parallel (0°) to the superlattice nanowire axis, the resonance field of the absorption peak is larger than that for the angle of 30°and 45°, but smaller than that for the angle of 60°and perpendicular (90°).

(a)

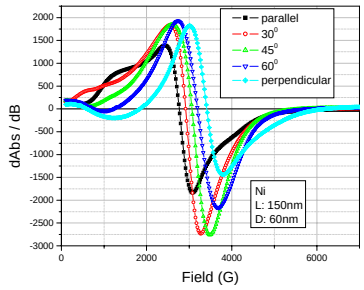

(b)

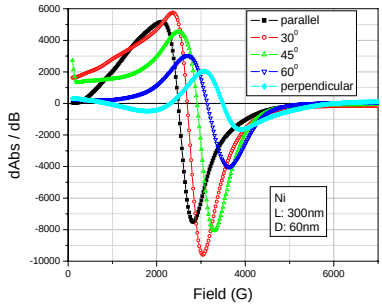

(c)

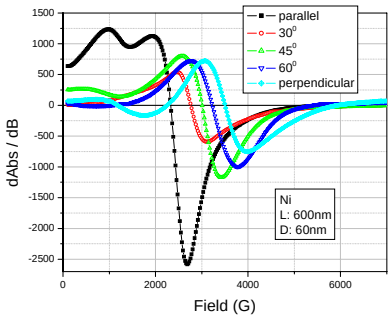

(d)

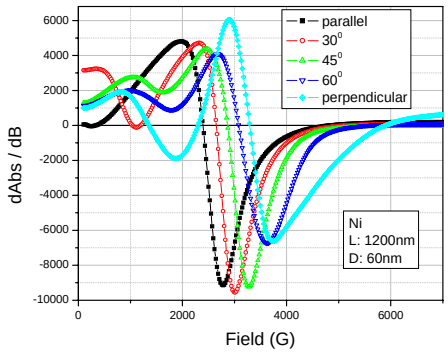

(e)

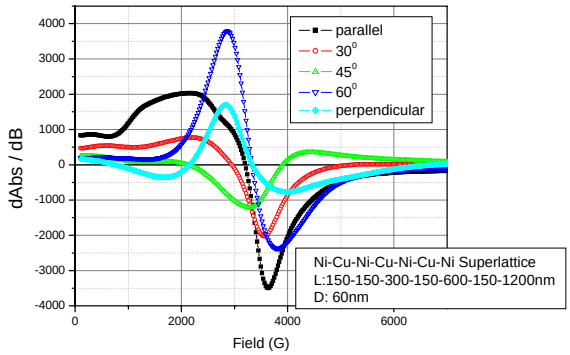

Figure 3.2 FMR spectra for a series of specimens of Ni nanowire arrays with different lengths (a , b , c , d) and Ni/Cu superlattice nanowire arrays (e); The sequence of FMR spectra at X-band (9.8Hz) were recorded as function of the angle between the applied external field and the nanowire axis

Figure 3.3 and Figure 3.4 are the FMR spectra of a series of Ni nanowire arrays of different lengths ranging from 150nm to 1200nm, which was recorded when the applied external field is parallel and perpendicular to the nanowire axis respectively. In those FMR spectra, only the sample with length of 600nm showed us a double of its spectra recorded when the applied external field is parallel to the nanowire axis, and all other sample with different length only have single absorption peak. Besides, the resonant field of absorption peak could be changed by changing the nanowire resulting in the varying of the aspect ratio, which showed us that these nanowire array samples' effective

demagnetizing factor can be turned by changing the nanowire aspect ratio. Besides, for the sample with same aspect ratio, the resonant field values of spectra for the applied external field parallel to the nanowire axis is smaller than those for the applied external field perpendicular to the nanowire axis, which is contributed from the effect of shape anisotropy.

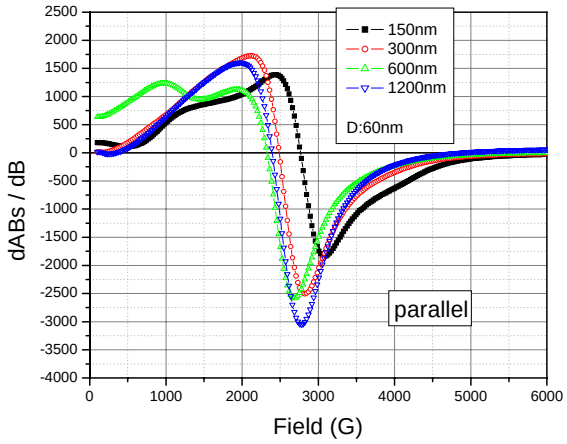

Figure 3.3 FMR spectra for a series of Ni nanowire arrays of different lengths were recorded when the applied external field is parallel to the nanowire axis

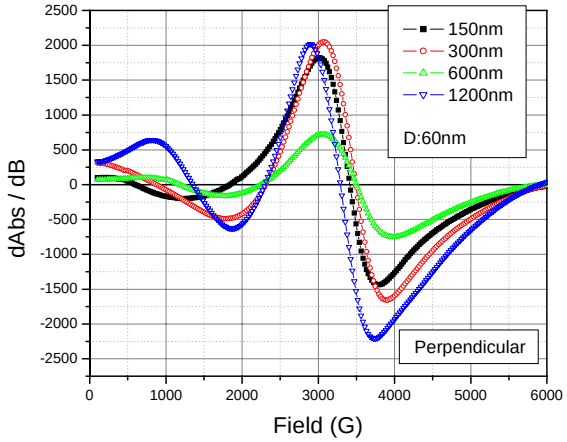

Figure 3.4 FMR spectra for a series of Ni nanowire arrays of different lengths were recorded when the applied external field is perpendicular to the nanowire axis

3.4 Conclusions

Vibrating Sample Magnetometer (VSM) and Ferromagnetic Resonance (FMR) were utilized to characterize the magnetic behaviors of Ni nanowire arrays of different lengths and Ni/Cu superlattice nanowire arrays. The VSM data exhibited that the magnetic easy axis of samples is parallel to the nanowire axis direction and the nanowire arrays have obvious shape anisotropy. The FMR spectra indicated that the resonant field value is angular and aspect ratio dependence.

References

[1]. Iijima, S. *Nature* **354**, 56 (1991).

[2]. Kroto, H.W., Heath, J.R., O'Brien, S.C., Curl, R.F.& Smalley, R.E. *Nature* **318**, 162-163 (1985)

[3]. Miller, D.A.B., Chemla, D.S., Damen, T.C., Gossard, A. C., and Wiegmann,W., Wood, T. H., and Burrus, C. A. *Phys. Rev. Lett.* **53**, 2173–2176 (1984)

[4]. Arakawa,Y., Sakaki, H. *Appl. Phys.Lett*. **40**, 939 (1982)

[5]. H. Drexler, D. Leonard, W. Hansen, J. P. Kotthaus, and P. M. Petroff, *Phys. Rev. Lett.* **73**, 2252 (1984)

[6]. S. Sauvage, P. Boucaud, F. H. Julien, J.-M. Gérard, and J.-Y. Marzin, *J. Appl. Phys.* **82**, 3396 (1997)

[7]. N. Kirstaedter, N. N. Ledentsov, M. Grundmann, D. Bimberg, V. M. Ustinov, S. S. Ruvimov, M. V. Maximov, P. S. Kop'ev, Zh. I. Alferov, U. Richter, P. Werner, U. Gösele, and J. Heydenreich, *Electron. Lett*. **30**, 1416 (1994)

[8]. M. Grundmann, J. Christen, N. N. Ledentsov, J. Bohrer, D. Bimberg, S. S. Ruvimov, U. Richter, P. Werner, U. Gosele, J. Heydenreich, V. M. Ustinov, A. Y. Egorov, A. E. Zhukov, P. S. Kop'ev, and Zh. I. Alferov, *Phys. Rev. Lett*. **74**, 4043 (1995)

[9]. A. P. Roth, P. Lévesque, R. W. G. Syme, D. J. Lockwood, G. C. Aers, T. S. Rao, and C. Lacelle, *J. Appl. Phys.* **80**, 4033 (1996)

[10] B. Lakshmi, B. J. Robinson, Daniel T. Cassidy, and D. A. Thompson, *J. Appl. Phys.* **81**, 3616 (1997)

[11]. R. Benzaquen, R. Leonelli, S. Charbonneau, *Phys. Rev. B.* **59**, 1973 (1999)

[12]. S. Privitera, F. La Via and C. Spinella, S. Quilici, A. Borghesi, and F. Meinardi, M. G. Grimaldi and E. Rimini, *J. Appl. Phys.* **88**, 7013 (2000)

[13]. Myung-Kwan Ryu, Seok-Min Hwang, Tae-Hoon Kim, and Ki-Bum Kim, Seok-Hong Min, *Appl. Phys. Lett.* **71**, 3063 (1997)

[14]. Y. Z. Hu, D. J. Diehl, Q. Liu, C. Y. Zhao, and E. A. Irene, *Appl. Phys. Lett*. **66**, 700 (1995)

[15]. Martin, C.R. *Science*. **266**, 1961 (1996)

[16]. Wang,L., Yu-Zhang, K., Metrot, A., Bonhomme, P., Troyon, M.. *Thin Solid Films.* **288**, 86 (1996)

[17]. Peng, L.Q., Ju, X., Wang, S.C., Xian, D.C., Chen, H., He, Y.J.. *Chinese Phys. Letters.* **16**, 126 (1999)

[18]. Hiruma, K., Yazawa, M., Katsuyama, T., Ogawa, K., Haraguchi, K., Koguchi, M., Kakibayashi, H.. *J. Appl. Phys.* **77**,447 (1995)

[19]. Frederick C. K. Au, K. W. Wang, Y. H. Tang, Y. F. Zhang, I. Bello, and S. T. Lee, *Appl. Phys. Lett*. **75**, 1700 (1999)

[20]. X. Zheng, G. H. Chen, Z. B. Li, S. Z. Deng, and N. S. Xu, *Phys. Rev. Lett*. **92**, 106803 (2004)

[21]. E. Comini, G. Faglia, G. Sberveglieri Z. W. Pan, and Z. L. Wang, *Appl. Phys. Lett*. **81**, 1869 (2002)

[22]. Z. S. Wu, S. Z. Deng, N. S. Xu, Jian Chen, J. Zhou, and Jun Chen, *Appl. Phys. Lett.* **80**, 3829 (2002)

[23]. Y. J. Chen, Q. H. Li, Y. X. Liang, and T. H. Wang, Q. Zhao and D. P. Yu, *Appl. Phy. Lett.* **85**, (23) 5682-5684 (2004)

[24]. Min-Hua Zhao, Zhong-Lin Wang,Scott X. Mao, *Nano Lett.* **4** (4), 587-590 (2004)

[25]. Q. H. Wang, A. A. Setlur, J. M. Lauerhaas, J. Y. Dai, E. W. Seelig, R. P. H. Chang, *Appl. Phys. Lett.* **72**, 2912-2913 (1998)

[26]. Ando, S., Fukui, T.. *J. Crystal Growth.* **98**, 646 (1989)

[27]. Karam, N.K., Mastrovito, A., Haven, V., Ismail, K., Pennycook, S., Smith, H.I.. *J. Crystal Growth.* **107**, 591 (1991)

[28]. Canham, L.T.. *Appl. Phys. Lett.* **57**, 1046 (1990)

[29]. H. Takagi, H. Ogawa, Y. Yamazaki, A. Ishizaki, and T. Nakagiri, *Appl. Phys. Lett.* **56**, 2379 (1990)

[30]. Heath, J.R., LeGoues, F.K.. *Chem. Phys. Lett.* **208**, 263 (1993)

[31]. Zhang, H.Z., Kong, Y.C., Wang, Y. Z., Bai, Z.G., Wang, J.J., Yu, D.P., Ding, Y., Hang, Q.L., Feng, S. Q.. *Solid State Commun.* **109**, 677 (1999)

[32]. Dai, H., Wong, E.W., Lu, Y.Z., Fan, S., Lieber, C.M.. *Nature.* **375**, 769 (1995)

[33]. Han, W.Q., Fan, S.S., Li, Q.Q., Liang, W.J., Gu, B.L., Yu, D.P., *Chem. Phys. Lett.* **265**, 374 (1997)

[34]. Han, W.Q., Fan, S.S., Li, Q.Q., Gu, B.L., Zhang, X. B., Yu, D.P. *Appl. Phys. Lett.* **71**, 2271 (1997)

[35]. 1. I. Huynen, G. Goglio, D. Vanhoenacker, and A. Vander Vorst, *IEEE Microw. Guided Wave Lett.,* **9**, 401-403 (1999)

[36]. O. Yalcin, F. Yildiz, M. Ozdemir, B. Aktas, Y. Koseoglu, M. Bal, and M. T. Tuominen, *J. Magn. Magn. Mater.*, 272-76, 1684-1685 (2004)

[37]. K. Liu, K. Nagodawithana, P. C. Searson, and C. L. Chien, *Phys. Rev. B.* **51**, 7381 (1995)

[38]. R. W. Chantrell, *J. Magn. Magn. Mater*. **95**, 365 (1991)

[39]. M. N. Baibich, J. M. Broto, A. Fert, F. Nguyen Van Dau, F. Petroff, P. Eitenne, G. Creuzet, A. Friederich, and *J. Chazelas, Phys. Rev. Lett.* **61**, 2472–2475 (1988)

[40]. W. P. Pratt, Jr., S.-F. Lee, J. M. Slaughter, R. Loloee, P. A. Schroeder, and J. Bass, *Phys. Rev. Lett.* **66**, 3060–3063 (1991)

[41]. Zheng M, Menon L, Zeng H, Liu Y, Bandyopadhyay S, Kirby R D and Sellmyer D *J Phys. Rev. B* **62,** 12282 (2000)

[42]. Wagner, R.S., Ellis, W.C.. *Appl. Phys. Lett.* **4**, 89 (1964)

[43]. Levitt, A.P., Whisker Technology, John Wiley & Sons, Inc.. P.25. (1970)

[44]. Sears, G. W.. *Acta Met.*. **1**, 367 (1953)

[45]. Sears, G. W.. *Acta Met.*. **3**, 457 (1955)

[46]. Melmed, A.J., Gomer, R.. *J. Phys. Chem.*. **34**, 1802 (1961)

[47]. Yu, D.P., Sun, X.S., Lee, C.S., Bello, I., Lee, S.T., Gu, H.D., Leung, K.M., Zhou, G.W., Dong, Z.F., Zhang, Z.. *Solid State Commun.* **105**, 403 (1998)

[48]. Yu, D.P., Bai, Z.G., Ding, Y., Hang, Q.L., Zhang, H.Z., Zou, Y.H., Wang, J.J., Qian, W., Zhou, H.T., Xiong G.C., Feng, S.Q.. *Appl. Phys. Lett.* **72**, 3458 (1998)

[49]. Yu, D.P., Hang, Q.L., Ding, Y., Zhang, H.Z., Bai, Z.G., Wang, J.J.,Zou, Y.H., Qian, W., Xiong, G.C., Feng, S.Q.. *Appl. Phys. Lett*. **73**, 3076 (1998)

[50]. Paunovic, M., Schlesinger. Fundamentals of Electrochemical Depostion. John Wily & Sons, Inc., U.S.A (1998)

[51]. O. Shinoura, S.Kamijo, K.Narumiya. *J. Mag. Soc. Jpn.* . **18,** 277 (1994)

[52]. Namaura, A., M. Takai, K. Hayashi, T. Osaka. *J. Surf. Finish. Soc. Jpn.*. **47**, 934 (1996)

[53]. G.E.Thompson, *Thin Solid Films* **297**, 192 (1997)

[54]. S.K.Chakarvarti, J.Vetter, Radiat. Meas. 29, 149 (1998)

[55] G.E.Possin, *Rev. Sci. Instrum.* **41**, 772 (1970)

[56] Xu, Y.J., Xu, D.S., Chen, D.P., Guo, G.L., Li, C.J.. *Acta Physicochimica Sinica.* **15**, 577 (1999)

[57]. Peter A. Smith, Christopher D. Nordquist, Thomas N. Jackson,Theresa S. Mayer, Benjamin R. Martin, Jeremiah Mbindyo, and Thomas E. Mallouk, *Appl. Phys. Lett.* **77**, 9 (2000)

[58]. P. Forrer, F. Schlottig, H. Siegenthaler, M. Textor, *Journal of Applied Electrochemistry.* **30**, 5 (2000)

[59]. X. Y. Zhang, L. D. Zhang, W. Chen, G. W. Meng, M. J. Zheng, and L. X. Zhao, *Chem. Mater.* **13**, 2511-2515 (2001)

[60]. WWW. WHATMAN.COM

[61] Wu, W., Cui,B., Sun, X., Zhang, W., Zhuang, L., Kong, L., Chou, S.Y. *J. Vac. Sci. Technol. B* **16**, 3825 (1998)

[62]. Masuda, H., Fukuda, K. *Science* **268**, 1466 (1995)

[63]. T.L. Wade, J-E. Wegrowe, Eur. Phys. *J.Appl. Phys.* **29,** 3-22 (2005)

[64]. Lowenheim, F.A.. Electroplating. Mcgraw-Hill, New York (1978)

[65]. Alper, M., K. Attenborough, R. Hart, S.J.Lane, D.S. Lashmore, C.Younes and W.Schwarzacher. *Appl. Phys. Lett.*. **63**, 2144 (1993)

[66]. Jessensky, O., Muller, F., Gosele, U. *Appl. Phys. Lett.* **72,** 1173 (1998)

[67]. Nielsch, K., Wehrspohn, R.B., Barthel, J., Kirschner, J. and Gosele, U. *Appl. Phys. Lett.* **79**, 1360 (2001)

[68]. Skomski, R.; Zeng, H.; Zheng, M.; Sellmyer, D. J. Phys. Rev. B. 65, 3900 (2000)

[69].Whitney, T.M.; Jiang, J.S.; Searson, P.C.; Chein, C.L. *Science.* **261**, 1316. (1993)

[70]. Wu, W.; Gui, B.; Sun, X.; Zhang, W.; Zhuang, L.; Kong, L.; Chou, S.Y. *J. Vac. Sci. Technol. B.* **16**, 3825 (1998)

[71]. Jessensky O, Müller F and Gösele U 1998 *Appl. Phys. Lett.* **72** 1173

[72]. A. Encinas-Oropesa, M. Demand, L. Piraux, I. Huynen, U. Ebels,. *Phys. Rev. B.* **63**, (10) 104 415 (2001)

Vita

Bo Ye was born in Shangyu, Zhejiang Province, a small historical town of eastern China. He entered Zhejiang Normal University, Jinhua, China in 1996 and got his B.S. degree in Chemistry in 2000. Then Bo Ye studied in Nano-bio-medicine Center at Shanghai Institute of Applied Physics, Chinese Academy of Sciences under the instruction of Dr. Wenxin Li from 2000 to 2003. He enrolled as a graduate student in the chemistry department at the University of New Orleans in Aug. 2003 and became a member of Dr. John B. Wiley's research group at the end of that year.